Int. J. Electrochem. Sci., 14 **(2019)** 5064 – 5074, doi: 10.20964/2019.06.08

International Journal of
ELECTROCHEMICAL
SCIENCE
www.electrochemsci.org

Electrochemical Behavior of Indium in LiCl-KCl Molten Salts

Peng Cui[1], *Bo Qin*[1,2,*], *Ana Maria Martinez*[3], *Geir Martin Haarberg*[4]

[1] Faculty of Metallurgical and Energy Engineering, Kunming University of Science and Technology, Kunming 650093, China;
[2] State Key Laboratory of Complex Nonferrous Metal Resources Clean Utilization, Kunming University of Science and Technology, Kunming 650093, China;
[3] SINTEF Materials and Chemistry, NO-7465 Trondheim, Norway;
[4] Department of Materials Science and Engineering, Norwegian University of Science and Technology, NTNU, NO-7491, Trondheim, Norway
[*]E-mail: 59077730@qq.com

Received: 7 January 2019 / *Accepted:* 18 March 2019 / *Published:* 10 May 2019

The electrochemical reduction processes were studied on glassy carbon electrode in molten LiCl-KCl eutectic at 450 °C. There is a consecutive two-step electrochemical process taking place to form metallic indium from the cathodic discharge of indium ions. The process is regarded as: $In^{3+} + 2e^- = In^+$ and $In^+ + e^- = In$. The diffusion coefficient of In^{3+} ion was determined by chronoamperometry. Mass transport towards the electrode is a simple diffusion process. Metallic indium is deposited on the glassy carbon electrode, which occurs at a potential of around -0.85 V vs. the Ag^+/ Ag reference electrode. $InCl_2$ forms InCl and $InCl_3$ disproportionately. After a certain time, the CV curves for $InCl_2$ and InCl were essentially the same as the one obtained from the reduction of $InCl_3$.

Keywords: Electrochemical behaviour, Indium chloride, Molten salts, Kinetic parameters

1. INTRODUCTION

Indium is an important metal material mainly used in electronics industry. It has no minerals of its own so that it has to be produced as a byproduct of other metallurgical processes. Indium is being identified as a critical metal because it is rare. Due to the scarcity and increasing demand for the metal, it is necessary to consider to separate and recycle indium from secondary sources. Recovery of indium from different sources is critical and helpful in the modern industry. The recovery of indium from waste sputtering targets and the obsolete LCDs have become more and more important because they are a valuable resource, and at the same time they are not environmentally friendly [1,2].

Several processes for recycling the waste LCD panels have been proposed, and are mainly based on solvent extraction [3-8], chemical precipitation [9-11] and pyrometallurgy – vacuum methods [12-14]. Bioleaching [15] and ultrasonic waves [16] are also applied in the indium leaching process. Molten salt electrolysis has been used for metal production for many years and is already a proven technology. There have been some electrochemical studies of indium ions in molten salts. Some researchers [17-19] observed that electroreduction occurred through only one electrochemical step related to the In (III)/In (I) couple, close to the cathodic limit involving a two-electron transfer. However, some other researchers [20-22] reported that there were two reversible electron exchange steps to form the intermediate species In (I) in the fused salts from the re-duction of $InCl_3$ solutions to indium metal. They also proved that InCl disproportionation occurred, yielding In and $InCl_3$.

In this work, the stability of the different valence states of indium were studied in the LiCl-KCl at 450 °C. This study is a part of a systematic research into the possibility of the recovery of Sn and In contained in ITO powder.

2. EXPERIMENTAL

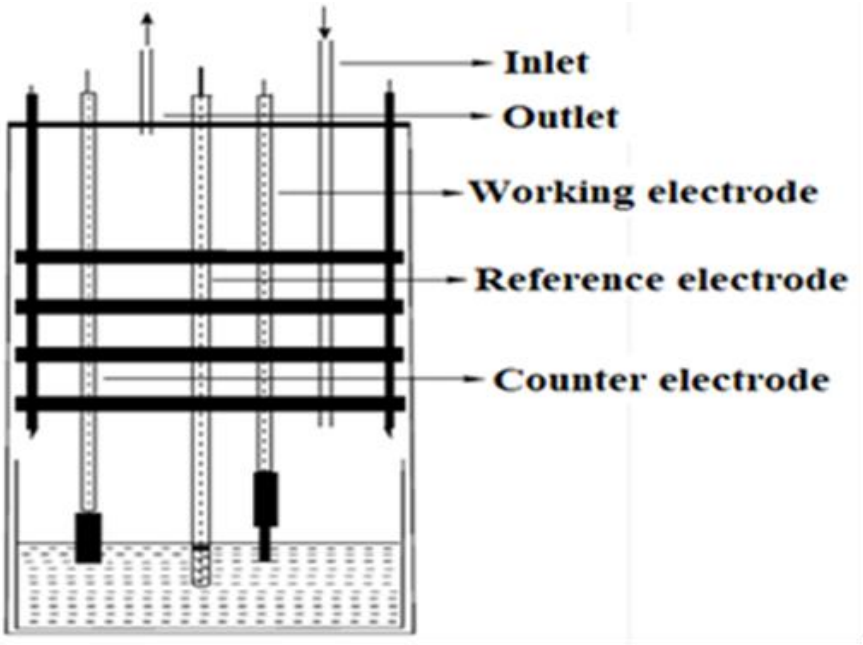

Figure 1. Schematic diagram of the electrochemical cell

Figure 1 show a picture and a schematic drawing of the electrochemical cell. The furnace was a vertical tube furnace controlled by at Eurotherm 902 controller. The tube was made of mullite, and on the top and bottom was water-cooled lids. The electrolyte was contained in a cylindrical pyrex glass or alumina crucible and was situated inside a gas-tight quartz container. At the top of the quartz tube a clamp fitted with 3 rubber O-rings ensured an air-tight assembly between the tube itself and the lid of the tube. There were 7 holes on the lid for the electrodes, temperature probe, gas and the feed tube. The experiments were performed under inert argon atmosphere. To minimize the temperature gradient, a total of 4 evenly spaced alumina radiation shields extended from the crucible up to the top of the tube.

The temperature in the cell was controlled with a Pt 10% Rh vs Pt thermocouple. A glassy carbon rod (3 mm) is used as a working electrode. The reference electrode is a silver wire with 0.75 mol·kg^{-1} AgCl and placed in the mullite ($3Al_2O_3 \cdot 2SiO_2$) tube. A graphite rod (8 mm) is used as a counter-electrode in the electrochemical studies. LiCl : KCl with the eutectic composition (58.2 : 41.8 mol%) was dried in a heating cabinet at 150 °C for at least 24 hours prior to the start of the experiments. In these experiments, 200 g of eutectic LiCl-KCl was used. After the salt had melted around 0.1 mol% metal chlorides were added. The voltammetry studies were performed with an Autolab PGSTA20 computer controlled potentiostat with a 10 A current booster unit connected computer controlled potentiostat.

3. RESULTS AND DISCUSSION

3.1 Study of indium electrodeposition from $InCl_3$ solutions

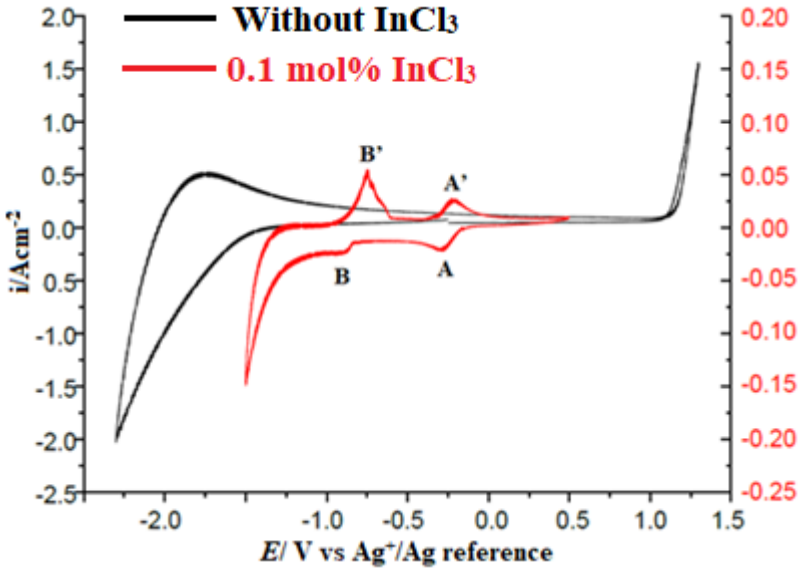

Figure 2. Cyclic voltammograms obtained at a glassy carbon in the molten LiCl-KCl at 450 °C with and without $InCl_3$. The potential is swept in the cathodic direction from the open circuit potential. Sweep rate is 100 mV/s

The reduction process on glassy carbon electrode in molten LiCl-KCl eutectic containing $InCl_3$ was studied by cyclic voltammetry. Results are shown in Fig 2. In the pure LiCl-KCl melt, in the anodic domains, the chlorine evolution was observed. During cathodic polarization, lithium intercalation into graphite occurred before deposition of metallic lithium was reported by Xu [23]. Here, metallic lithium deposition started was later than lithium intercalation into glassy carbon occurred. When adding $InCl_3$ to a pure LiCl-KCl eutectic melt, two red/ox couples corresponding to two electrochemical processes were detected at a glassy carbon, A/A' and B/B'. The cathodic wave A associated with the anodic wave A' are related to the In^{3+}/In^{+} exchange. Their shapes are characteristic of a soluble-soluble exchange. This wave occurs from -0.14 V. The cathodic peak B and the anodic stripping peak B' are characteristic of a system involving an insoluble product which corresponds to the In^{+}/ In system. Metallic indium deposition on the glassy carbon electrode can be seen from the position where the cathodic current B increases, which occurs at a potential of around -0.85 V.

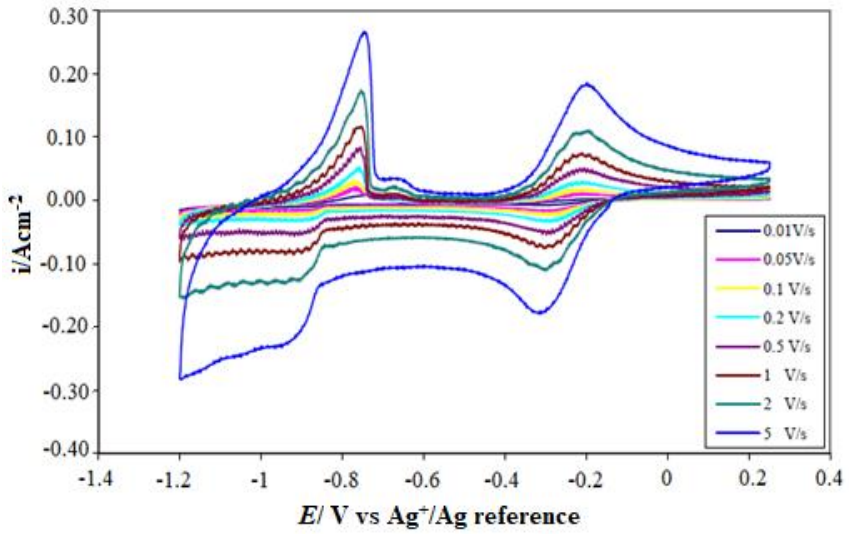

Figure 3. Cyclic voltammograms of the reduction of $InCl_3$ in the molten LiCl-KCl at 450 °C at different sweep rates by a glassy carbon electrode

A series of voltammograms for the reduction of $InCl_3$ recorded with a glassy carbon electrode in a wide scan rate range is presented in Fig 3. There are two steps for the redox reaction of indium ions. The peak current densities increase with the sweep rate. The shapes of the peaks become analogous to a diffusion peak for the In^{3+}/In^{+} exchange. The two reduction peak potentials don't vary with sweep rate. It is noticed that there is a slight anodic wave between the two obvious anodic peaks. It is an indication that surface processes may be involved corresponding to desorption of liquid indium.

3.2 Study of In^{3+}/In^{+} exchange

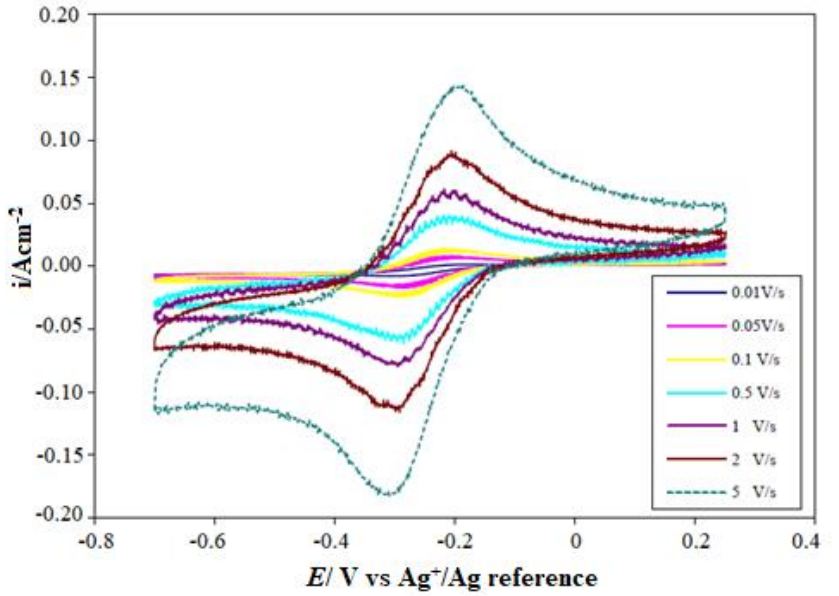

Figure 4. Cyclic voltammograms of A/A' in the molten LiCl-KCl at 450 °C at different sweep rates by a glassy carbon electrode

To study the electrochemical behaviour of the A/A' system, cyclic voltammograms were recorded from + 0.2 V to - 0.7 V potential range. The peak couple A/A' was investigated by cyclic voltammetry at different sweep rates as shown in Fig 4. As the sweep rate is increased a peak of increasing height develops. A number of parameters can be extracted from such i-E curves, some of which are included in Table 1. E_p is independent of v.

Table 1. Data obtained by analysing voltammograms of peak couple from the figure 4 for different sweep rates

v [V/s]	i_p^c [A/cm^2]	E_p^c [V]	$E_{p/2}^c$ [V]	n
0.01	-0.01	-0.31	-0.22	1.55
0.05	-0.02	-0.30	-0.22	1.71
0.1	-0.02	-0.30	-0.23	2.00
0.5	-0.06	-0.29	-0.22	2.22
1	-0.08	-0.29	-0.22	1.93
2	-0.12	-0.30	-0.23	1.89
5	-0.18	-0.31	-0.23	1.69

The number of electrons transferred was calculated by using the difference between the peak and half peak potentials as given in equation (1). The average number of electrons for the first step was determined to be 2 from the data in Table 1.

$$/E_p\text{-}E_{p/2}/=2.2RT/nF \quad (1)$$

The peak couple A/A' corresponding to the In (I)/In (III) was confirmed as well as B/B' corresponding to the In/In(I) in Fig 2. Therefore, there is a consecutive two-step electrochemical process taking place to form metallic indium from the cathodic discharge of indium ions. The process is regarded as:

$$In^{3+}+2e^- = In^+ \quad (2)$$

$$In^++e^- = In^0 \quad (3)$$

The cathodic peak current density i_p of the first cathodic peak was determined and plotted versus the square root of the sweep rate, which is shown in Fig 5. A plot of i_p against $v^{1/2}$ yields a straight line passing through the origin with the slope 0.081. The result indicates that the transport of the electroactive species at the surface of the electrode was controlled by the diffusion of In^{3+} species. The value of $D_{In^{3+}}$ is 1.14×10^{-5} cm$^2\cdot$s^{-1} deduced from Randles-Servcick equation (4) that can be employed when both the reactant and product are soluble:

$$I_p = 0.4463\, n^{3/2} F^{3/2} A(RT)^{-1/2} D^{1/2} C_0 v^{1/2} \quad (4)$$

where I_p is the peak current (A), A the surface area of working electrode (cm^2), D the diffusion coefficient (cm$^2\cdot$s^{-1}), C_0 the bulk concentration of the species (mol$\cdot$cm^{-3}), 0.0000495 mol/cm^3 and v the sweep rate (V$\cdot$s^{-1}).

It is also possible to calculate the diffusion coefficient for the In^{3+} ion from chronoamperometry. The curves with different applied potentials (- 0.25 ~ - 0.8 V) were obtained as shown in Fig 6. With increasing applied potentials the current maximum increases. Then the limiting current was determined

as a function of time by plotting current versus potentials at various times (4 s - 10 s) from the current transients.

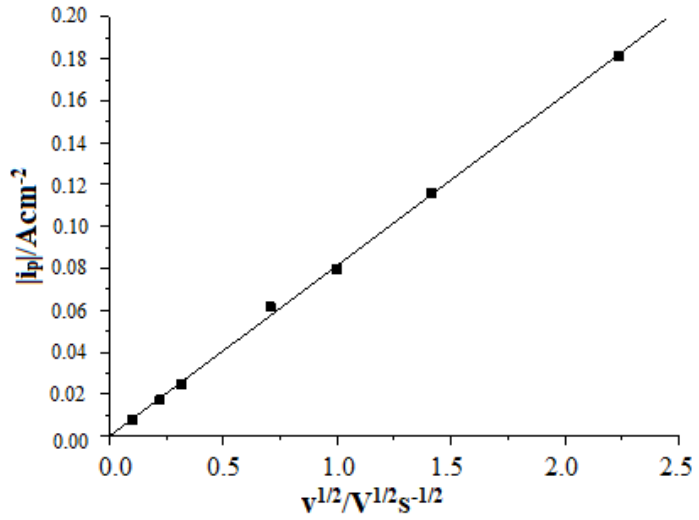

Figure 5. Variation of the In (III)/(I) peak current density with $v^{1/2}$

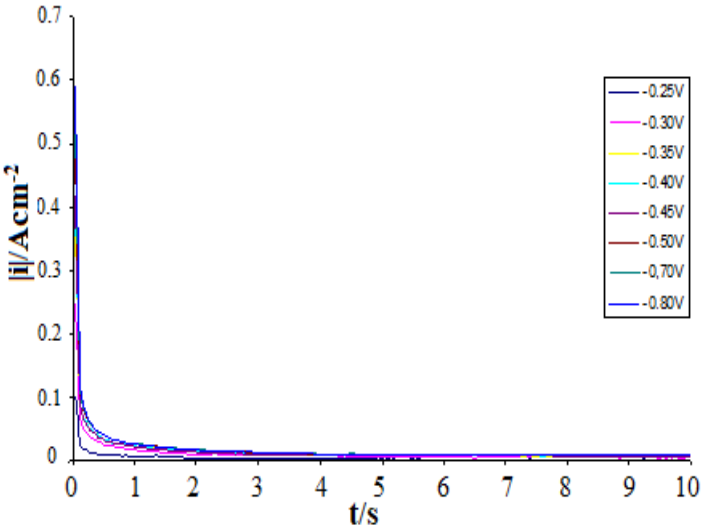

Figure 6. Chronoamperometric response curses obtained for different potential steps

A plot of i against $t^{-1/2}$ is linear and passes through the origin thus the process is diffusion controlled. The diffusion coefficient can be calculated from the slope according to the Cottrell equation

$$i = -\frac{nFD^{1/2}c_O^{\infty}}{\pi^{1/2}t^{1/2}} \quad (5)$$

Limiting current density for In (III) falls as $t^{-1/2}$ as shown in Fig 7. From the slope -0.017, the diffusion coefficient D_{In}^{3+} is determined to be 1.02×10^{-5} $cm^2\cdot s^{-1}$. The diffusion coefficient obtained by CA is a little lower than the one measured by CV. The In (III) diffusion coefficient was calculated from the plateau of the convoluted voltammograms [21], which is D_{In}^{3+} is 1.3×10^{-5} $cm^2\cdot s^{-1}$ in the LiCl-KCl

eutectic at 450 °C. The differences between these values are mainly related to the difficulty in determining the exact active electrode area.

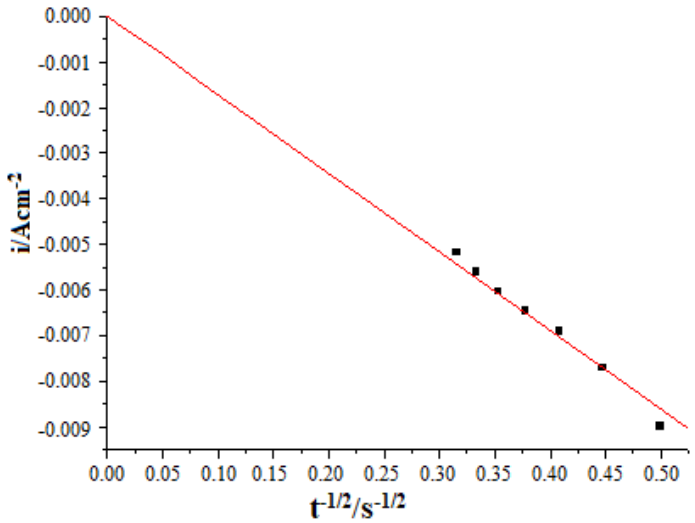

Figure 7. Limiting current density for In (III) versus $t^{-1/2}$

Therefore, it is possible to observe very good agreement between the different techniques employed. Comparing with Castrillejo's work [24], The In (III) diffusion coefficients D_{In}^{3+} are 6.5 ± 0.2×10^{-6} $cm^2 \cdot s^{-1}$ and 6.0 ± 0.2×10^{-6} $cm^2 \cdot s^{-1}$ on tungsten by voltammetry and chronopotentiometry respectively. In^{3+} ion even has a larger diffusion coefficient in molten LiCl-KCl at 450 °C than that in molten equimolar $CaCl_2$-NaCl mixture at 550 °C.

3.3 Study of In^{2+} and In^{+} stability

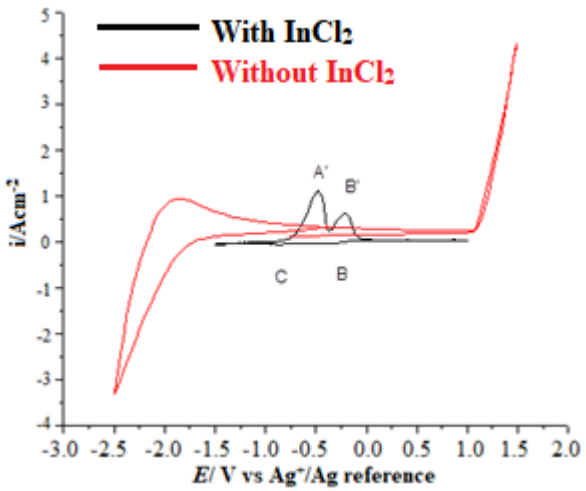

Figure 8. Cyclic voltammograms of the reduction of $InCl_2$ in the molten LiCl-KCl at 450 °C with and without $InCl_2$. The potential is swept in the cathodic direction from the open circuit potential.

The standard free energy ΔG^{θ} for the disproportionation reaction (6) is almost zero at 450 °C and becomes negative above 450 °C [25]. Pure molten $InCl_2$ is not stable at high temperatures and should form InCl and $InCl_3$ disproportionately. This is consistent with the following experiments.

$$2InCl_2 \rightarrow InCl + InCl_3 \quad (6)$$

Fig. 8 shows the cyclic voltammograms of the reduction of $InCl_2$ in the molten LiCl-KCl at 450 °C with and without $InCl_2$. After adding $InCl_2$, in the anodic direction, a new peak A' occurs. This is not corresponding to the depletion of In according to the position of the peak. So In^{2+} is probably oxidized to In^{3+}. The red/ox reaction B /B' corresponds to In^{+}/In^{3+}.

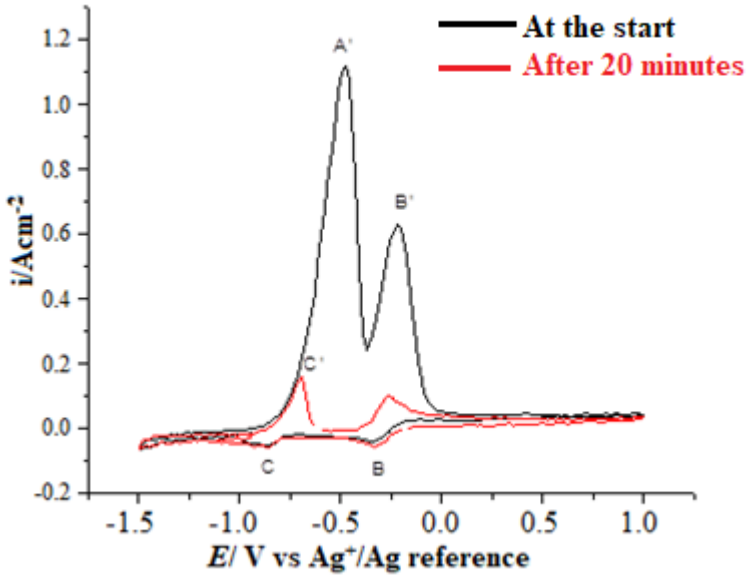

Figure 9. Cyclic voltammograms of the reduction of $InCl_2$ in the fused LiCl-KCl at 450 °C at different times by a glassy carbon electrode

After a short time, the peak A' disappeared and new peak C' which corresponding to In^{3+}/In^{+} exchange was observed in Fig 9. This means that In^{2+} is not stable, and the reaction (6) takes place. Raman spectra obtained from $InCl_2$ indicate that it exists in the pure melt as In^{+} $(InC1_4)^{-}$ and in a chloride melt as a mixture of $InCl_4^{-}$ and $InCl_5^{2-}$ [26]. The Raman evidence establishes that $InCl_2$, in the liquid state, and probably also in the solid, has the structure $In^{+}InCl_4^{-}$ [27].

Many voltammograms of the reduction of $InCl_2$ to indium at a glassy carbon electrode at 450 °C are shown in Fig 10. The curves were practically the same as the one obtained from the reduction of $InCl_3$. The standard Gibbs free energy ΔG^{θ} for reaction (7) is positive 89.109 kJ at 450 °C. And the ΔG^{θ} value increases as the temperature increases. The equilibrium constant K^{θ} is 3.6×10^{-7} related to the standard Gibbs free energy change. This means the InCl is stable and hard to disproportionate, and the disproportionation phenomenon was not observed in these experiments.

$$3InCl \rightarrow 2In + InCl_3 \quad (7)$$

They observed the disproportionation of InCl in the fused LiCl-KCl eutectic. They observed the In^{+}/In^{3+} redox process by direction of InCl pellets to the molten salt with scan starting in the cathodic

direction. The frozen samples of the solution by x-ray analysis showed that the InCl disproportionation occurred to yield In and $InCl_3$. In Clarke's study [27], it was suggested that the failure of sufficient Indium metal to dissolve for producing the InCl stoichiometry could be explained the tendency of In^+ to disproportionate according to the equation (7) in the presence of excess chloride. Liu [28] also observed the disproportionation of InCl to In^0 and In^{3+} in basic chloroaluminate molten salts. Further experiments are needed to study the stability of the monovalent anion In^+.

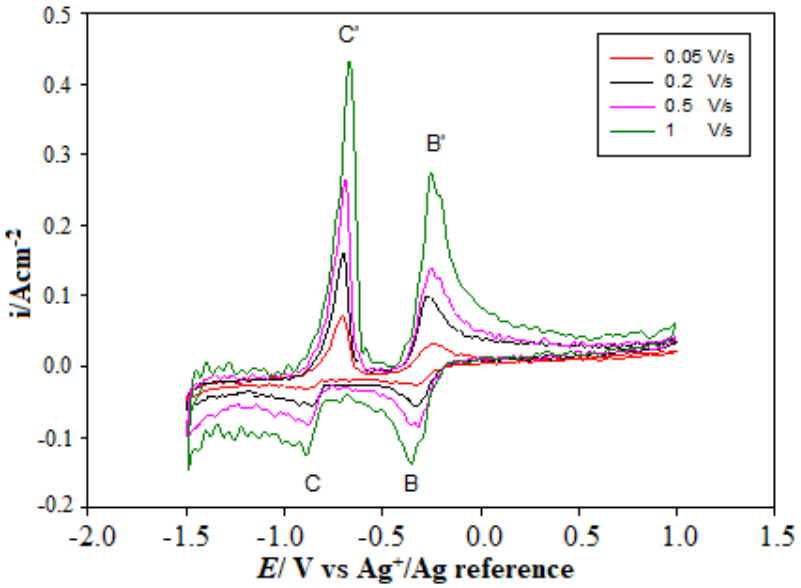

Figure 10. Cyclic voltammograms of the reduction of $InCl_2$ in the molten LiCl-KCl at 450 °C at different sweep rates by a glassy carbon electrode

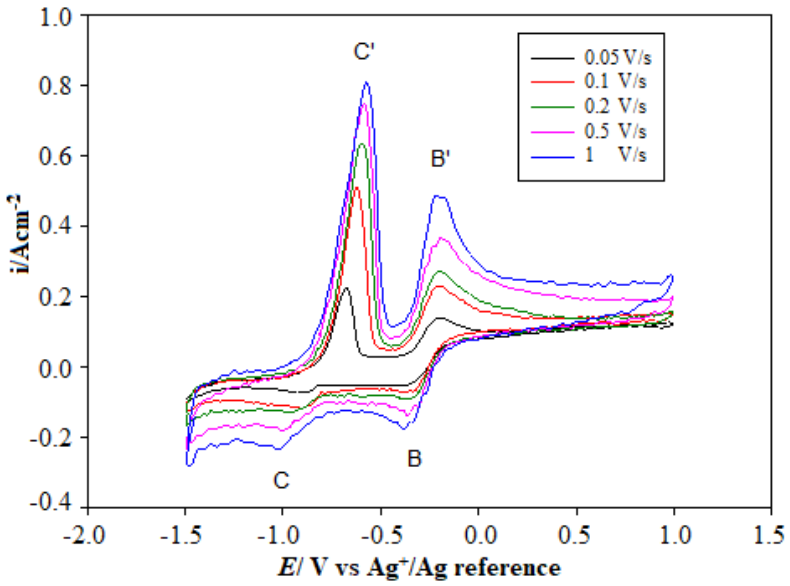

Figure 11. Cyclic voltammograms of the reduction of InCl in the molten LiCl-KCl at 450 °C at different sweep rates by a glassy carbon electrode

A series of voltammograms corresponding to the oxidation and reduction of InCl obtained at 450 °C for sweep rates from 0.05 up to 1 V/s is reported in Fig 11. The reversibility was the same with the test for $InCl_3$ described before.

4. CONCLUSIONS

There is a consecutive two-step electrochemical process taking place to form metallic indium from the cathodic discharge of indium ions. The onset of the reduction of In^{3+} occurs from -0.14 V. Metallic indium deposition occurs at a potential of around -0.85 V on the glassy carbon electrode. This process is regarded as: $In^{3+} + 2e^- = In^+$ and $In^+ + e^- = In$. The diffusion coefficient for In^{3+} was 1.0×10^{-5} $cm^2\cdot s^{-1}$ and 1.1×10^{-5} $cm^2\cdot s^{-1}$ respectively obtained by CA and CV. $InCl_2$ is not stable and disproportionate easily to form InCl and $InCl_3$.

ACKNOWLEDGMENTS
The research work was financially supported by Norwegian University of Science and Technology, Yunnan Province Science bureau of China (No. 2017FB083) and Kunming University of Science and Technology (No. KKSY201652048).

References

1. A. Weiser, D.J. Lang, T. Schomerus, A. Stamp, *J. Clean. Prod.,* 94 (2015) 376.
2. G. Dodbiba, H. Nagai, L.P. Wang, K. Okaya, and T. Fujita, *Waste Manage.,* 32 (2012) 1937.
3. W.S. Chou, Y.H. Shen, S.J. Yang, T.C. Hsiao, L.F. Huang, *Environ. Prog. Sustainable Energy.,* 35 (2016) 758.
4. J. Yang, T. Retegan, and C. Ekberg, *Hydrometallurgy*, 137 (2013) 68.
5. S. Gu, B. Fu, G. Dodbiba, T. Fujita and B. Fang, *RSC Adv.,* 7 (2017) 52017.
6. E.B. Pereira, A.L. Suliman, E.H. Tanabe, D.A. Bertuol, *Miner. Eng.,* 119 (2018) 67.
7. E. Torre, E. Vargas, C. Ron and S. Gamez, *Metals.,* 8 (2018) 776.
8. L. Rocchetti, A. Amato, F. Beolchini, *J. Clean. Prod.,* 116 (2016) 299.
9. M. Martin, E. Janneck, R. Kermer, A. Patzig, S. Reichel, *Miner. Eng.,* 75 (2015) 94.
10. D. Fontana, F. Forte, R. De Carolis, M. Grosso, *Waste Manage.,* 45 (2015) 325.
11. A.V.M. Silveira, M.S. Fuchs, D.K. Pinheiro, E.H. Tanabe, D.A. Bertuol, *Waste Manage.*, 45 (2015) 334.
12. S. Itoh, K. Maruyama, *High Temp. Mater. Processes.*, 30 (2011) 317.
13. H. Liu, Q. Wei, D. Liu, B. Yang, and Y. Dai, *J. Vac. Sci. Technol. A.,* 32 (2012) 902.
14. Y. He, E. Ma, and Z. Xu, *J. Hazard. Mater.*, 268 (2014) 185.
15. J. Willner, A. Fornalczyk, B. Gajda, M. Saternus, *Physicochem. Probl. Miner. Process.,* 54 (2018) 639.
16. K. Zhang, B. Li, Y. Wu, W. Wang, R. Li, Y.N. Zhang, T. Zuo, *Waste Manage.,* 64 (2017) 236.
17. Y. Castrillejo, M.A. Garcia, E. Barrado, P. Pasquier, and G. Picard, *Electrochim. Acta.,* 40 (1995) 2731.
18. H.A. Laitinen, C.H. Liu, and W.S. Ferguson, *Anal. Chem.,* 30 (1958) 1266.
19. M. Mohamedi, S. Martinet, J. Bouteillon, and J.C. Poignet, *Electrochim. Acta.*, 44 (1998) 797.
20. M.J. Barbier, J. Bouteillon, and M. Taoumi, *J. Electrochem. Soc.,* 133 (1986) 2502.
21. J. Bouteillon, M. Jolarian, J.C. Poignet, and A. Reydet, *J. Electrochem. Soc.,* 139 (1992) 1.
22. U. Anders and J.A. Plambeck, *Can. J. Chem.,* 47 (1969) 3055.

23. Q. Xu, C. Schwandt, G.Z. Chen, D.J. Fray, *J. Electroanal. Chem.*, 530 (2002) 16.
24. Y. Castrillejo, M.R. Bermejo, A.M. Martínez, C. Abejón, S. Sánchez, G.S. Picard, *J. Appl. Electrochem.,* 29 (1999) 65.
25. I. Barin, O. Knacke, O. Kubaschewski, Thermochemical properties of inorganic substances: supplement, Berlin Springer-Verlag, (1977), New York, America.
26. J.T. Kenney and F.X. Powell, *J. Phys. Chem.,* 72 (1968) 3094.
27. J.H.R.Clarke and R.E.Hester, *Chem. Commun.,* (1968) 1042.
28. J.S.Y. Liu and I.W. Sun, *J. Electrochem. Soc.,* 144 (1997) 140.